Influence of Water Cooling and Post-Weld Ageing on Mechanical and Microstructural Properties of the Friction-Stir Welded 6061 Aluminium Alloy Joints

Article *in* Applied Mechanics and Materials · February 2018

DOI: 10.4028/www.scientific.net/AMM.877.163

CITATIONS
40

READS
818

4 authors:

Venkateswarlu Devuri
Marri Laxman Reddy Institute of Technology
58 PUBLICATIONS **779** CITATIONS
SEE PROFILE

Murali Mohan Cheepu
Pukyong National University
100 PUBLICATIONS **1,458** CITATIONS
SEE PROFILE

Krishnaja Devireddy
Institute of Aeronautical Engineering
3 PUBLICATIONS **122** CITATIONS
SEE PROFILE

S. Muthukumaran
National Institute of Technology Tiruchirappalli
98 PUBLICATIONS **1,384** CITATIONS
SEE PROFILE

Applied Mechanics and Materials
ISSN: 1662-7482, Vol. 877, pp 163-176
doi:10.4028/www.scientific.net/AMM.877.163

Submitted: 2017-08-17
Revised: 2017-08-26
Accepted: 2017-09-03
Online: 2018-02-15

Influence of Water Cooling and Post-Weld Ageing on Mechanical and Microstructural Properties of the Friction-Stir Welded 6061 Aluminium Alloy Joints

D. Venkateswarulu[1,a]*, Muralimohan Cheepu[2,b], Devireddy Krishnaja[3,c] and S. Muthukumaran[4,d]

[1]Department of Mechanical Engineering, Marri Laxman Reddy Institute of Technology and Management, Telangana 500043, India

[2]Department of Mechatronics Engineering, Kyungsung University, Busan 48434, Republic of Korea

[3]Department of Mechanical Engineering, Institute of Aeronautical Engineering, Telangana 500043, India

[4]Department of Metallurgical and Materials Engineering, National Institute of Technology Tiruchirappalli, Tamil Nadu 620015, India

[a]dvriitr@gmail.com, [b]muralicheepu@gmail.com, [c]krishnaja8003@gmail.com, [d]smuthu@nitt.edu

Keywords: Friction stir welding, under water welding, PWHT, aluminum alloys, mechanical properties, microstructure

Abstract. A 6061-T6 aluminium alloy was friction stir welded in submerged water as well as in air cool at a constant traverse speed and different rotational speed in order to investigate the microstructural characterization and mechanical behaviour of the joints. In order to improve the tensile strength of the joints, weldments were studied at different heat treatment processes such as post weld aged condition and solutionized condition. It is observed that, water cooled joints are resulted in enhancing of both strength and ductility with the lower strain hardening ability than the air cooled joints. The width of the hardness distribution varies with the different cooling process of the joints. The highest hardness peak observed to be located in the heat affected zone of the joints. The maximum tensile strength of the joints achieved for welds under water cooled conditions in contrast to air cooled conditions. Moreover, a combination of water cooling and post weld ageing is proven to be the optimal path to improving the microstructural and mechanical properties of the joints with a maximum efficiency of 89.87% of the base metal strength. The microstructural observations of the joints revealed the presence of voids defects for the low rotational speed joints due to the insufficient heat input. The nugget of the higher tensile strength joints were free from defects and showed the fine grained material flow patterns which are constructive to obtain better mechanical properties.

Introduction

The joining of aluminum and its alloys has continuously constituted a prodigious challenges for design engineers and manufacturing technologists. The most commonly used metals are aluminium, magnesium, titanium, steel and their alloys for aircraft constructions. Although, its lighter weight than steel, which helps increase load carrying capacity and reduce power requirements, low maintenance and excellent corrosion resistance [1]. The specific strength of aluminium alloys is about three times that of normal structural steels. Due to their, light weight it is most suitable material for aircraft structures thus, possible to increase the cargo load and to reduce fuel consumption. Aluminum alloys which are widely used in various industrial applications other than aerospace, such as heat-treatable aluminum alloys are facing difficulties to weld by conventional fusion welding processes. During welding, due to the generation of high temperatures some welding defects such as porosity and cracks are certainly formed in the fusion zone [2]. In addition to this, fusion welding techniques often lead to substantial strength deterioration in the welded joint owing

to changes in metallurgical properties of the joints in fusion zone and heat affected zone. In order to overcome these problems solid state welding processes such as friction welding [3-8], ultrasonic welding [9], diffusion welding [10], friction stir welding [11-17], and explosive welding [18] are contemplated. Although, the solid state welding techniques have performed better than fusion welding techniques, still these are not able to produce a quality joints in case of dissimilar combinations of aluminum to titanium, stainless steel, magnesium, and any combinations of these alloys. To achieve reliable joints a new method has been implemented using of interlayers such as copper [19] and nickel [20-24]. However, solid state welding process of friction stir welding process represents a valid choice in order to produce a high reliable joints without any problems for all materials combinations in contrast to other welding processes.

Friction stir welding (FSW) is a new solid state welding process developed by The Welding Institute in the 1990s [25]. It is a solid-state joining technique, initially used for joining of aluminium alloys successfully. In recent years, FSW is being attractive joining method to the automotive, aerospace, shipbuilding and cargo industries, and it is fascinating a continuous demands in amount of research in interest to make the developments in the process. FSW comprises the advancing of a rotating tool along the abutting surfaces of two substrates. The friction between the substrates and tool generates the heat which is in effect of extruded around the tool materials before the tool shoulder touches and forging. The final weld is made with deforming the substrates material at joint temperatures lower than the melting point, and thus, it is possible to evade many of the welding defects and environmental effects related with fusion welding operations [26]. FSW can be feasible to joining of various materials that are not possible or difficult to join by fusion welding techniques. The friction stir welding tool is a crucial part of this welding operation accordingly, mechanical properties and microstructural characteristics of the FSW welded materials can be affected by various factors such as welding conditions, material composition, microstructures of the before and after welding, and various geometric parameters of the friction stir welded tool and the substrates [27, 28]. In this regard, the maximum temperature is observed in the weld stir zone, which influence the changes the precipitate distribution in the base material and also due to mixing of the plasticized material during tool rotation. The presence of changes in the temperature and heat distribution during welding can amend the ductility and strength of the FSW joints [29]. Initially various investigations were conducted on FSW of aluminium alloys including AA6061 to evaluate the effect of process parameters on microstructural, mechanical properties, and thermal analysis during and after FSW. Numerous researchers have been reported on recent developments in process parameters optimization, modelling, microstructure analysis and various applications of the FSW process. Microstructural characteristics of the welds has major impact on the joint strength and the detailed investigations of the various issues of FSW of AA6061-T6 were observed under transmission electron microscopy and light metallography procedures [30].

It is very important to understand the comparison of strength of the FSW joints with the conventionally fusion welding joints, and the previous studies were reported that the tensile strength of the AA6061 joints which are fabricated by gas tungsten arc welding, gas metal arc welding friction stir welded joints showed the maximum strength obtained for FSW welded joints due to the formation of very fine equi-axed grains which are uniformly distributed in the weld region are influences as a very fine strengthening precipitates [31]. Lim et al. [32] have investigated the influence of tool travel welding speed on mechanical properties of AA6061-T651 and reported that a decreasing of welding speed or an increase in rotating speed are resulted in low ductility welded joints owing to the gathering of coarse Mg_2Si particles in the FSW weld zone. Other studies on friction stir welding joints after heat treatment to evaluate the microstructural and mechanical properties have been carried out. In particular, aluminum alloys 2xxx and 6xxx-series alloys were friction stir welded widely for various applications and compared the joint properties in as weld condition and after post-weld heat treatment conditions. It was found that the post-weld heat-treatment (PWHT) friction stir welds of AA6061 was carried out at solutionizing temperatures in order of 520, 540, and 560 °C followed by ageing at two different temperatures of 175 °C and 200 °C. It was observed that the weld region (stir zone) showed very coarse grains after the PWHT.

The weldments hardness was distributed uniformly across the cross section after the PWHT. The bending of the samples failed after PWHT in root of the joints. However, the heat treatments conditions reduced the grain size but did not effect on the brittleness of the joints. The observance of little brittleness was recognized to the because of precipitate free zones surrounding to the grain boundaries and the equiaxed grain structure of the FSWed microstructure. The fracture analysis of the joints exhibited the failure was owing to the ductile inter-granular fracture mode [33]. The similar studies have been conducted on 2219-T87 friction stir welded joints and showed that the highest fatigue performance in contrast to electron beam welding process and gas tungsten arc welded joints. The achievement of such a high strengths were due to the formation of very fine, deformed grains and equally uniform distribution of precipitates in the weld region [34]. Later on the studies on influence of temper designations on friction stir weldability of AA6061 alloy have been reported and found that the sound joints were produced for AA6061 Al-alloy plates both in "O" and "T6" temper conditions. It is also found that the "O" temper condition exhibited a highest hardness in the weld region compared to the "T6" temper conditions [35]. Their further investigations on effect of post-weld heat treatment on the friction stir butt-joined AA6061 Al-alloy of "O" and "T6" temper conditions are studied in detailed microstructural investigations, hardness and transverse tensile testing. It was found that the PWHT FSWed joints results in formation of abnormal grain growth in the weld microstructure especially in the "O" temper condition. It is also observed that "O" temper condition depending on the welding conditions used in friction stir welding. In general PWHT can lead to an improvement in the strength of the joints even if abnormal grain growth can occur. The effect of post-weld heat-treatment on joints exhibited a higher mechanical properties than those of relevant as-welded samples and comparable to those of the respective base materials [36]. Zhang et al. [37] have been reported the effect of water cooling on friction stir welding of aluminum alloys heat affected zone microstructures. In their studies it was found that the hardness of the underwater joints improved drastically compared to the air cooling joints of heat affected zone. The results of hardness increase of heat affected zone were influenced the increasing of strength of the underwater joints. It is also investigated that, the controlling of thermal cycles of welded joint under water cooling had the intrinsic reason for the changes in microstructures and mechanical properties of the heat affected zone.

Although friction stir welding joints yields better properties compared to conventional fusion welding processes, but large variation in base metal strength to weld metal for various applications lead to increase in cost. If the strength of the friction stir welded joints can be further increased by some means it will be more advantageous for manufacturing sector. However, there are several studies conducted on different aspects of FSW of heat treatable aluminum alloys, there is still need a detailed studies on further develops on welding process, changes in mechanical properties and microstructure of the AA6061 alloys after welding as a result of subsequent heat treatment process. There are very few literature studies available on underwater welding of aluminum alloys and subsequently the effect of heat treatment on underwater welded joints properties and comparison to air cooling joints. The objectives of this research are to investigate the effects of welding conditions on underwater welding and air cooling welding joints mechanical and microstructural characteristics of the similar materials combinations of AA6061 alloys. Consequently, the mechanical properties and microstructural variations of the FSWed alloys in as welded conditions and post-welded conditions are assessed by means of hardness and tensile tests.

Experimental Procedure

The experiments were carried out using vertical milling machine for friction stir welding of aluminium plates. The base material utilized in the present study was 6061 aluminium alloy plate with the thickness of 6 mm. The chemical composition of the base material is given in Table 1. The friction stir welding was carried out using modified vertical milling machine which can able to control the required process parameters. Before welding, the edges of the base materials were machined to avoid the misalignments and cleaned with steel wire brush to remove the oxide layers and finally cleaned with alcohol to remove the dirt, oil, grease, etc.

Table 1 Chemical composition of the base material used in the present study (wt. %).

Al	Si	Fe	Cu	Mg	Mn	Ti	Zn	Cr
Balance	0.8	0.7	0.40	0.15	1.2	0.15	0.25	0.35

Table 2 Tool dimensions and process parameters used in the present study.

Rotational speed (rpm)	Traverse speed (mm/min)	Tool length (mm)	Pin length (mm)	Pin diameter (mm)
1120	32	75	5.8	3
1400				

Friction stir welding was carried out in air and water cooling (under water), respectively. The plates were clamped firmly in the jig to the backing plate in butt joint configuration, as shown in Fig. 1. The setup fixed in the vessel for under water welding, then vessel filled with water at room temperature to immerge the samples in water. FSW was performed in the longitudinal direction of the plates for air cooling and water cooling experiments using same tool and welding parameters. To achieve the proper welding procedure, friction stir welding tool was made by tool steel material with the size of 16 mm shoulder diameter and a M6 standard threads were machined on the pin, is shown in Fig. 2. To understand the range of welding conditions, numerous welds were performed using trial and error method. Based on the results of preliminary studies a range of welding conditions were optimized. The friction stir welding was done at the tool rotating speed of 1120 rpm and 1400 rpm, and transfer speed of 32 mm/min and other parameters are shown in Table 2. The photograph of the friction stir welding of water cooled and samples are illustrated in Fig. 3.

After the completion of welding, FSWed joints were sliced perpendicular to the welding direction using electrical discharge cutting machine for macro-structural studies and tensile tests. The cross-sectioned samples were prepared for microstructural analysis as per the ASTM E3-11 standard metallographic procedure. To reveal the microstructural features, samples were etched with tucker's reagent (4.5 ml HNO_3, 2.5 ml H_2O, 1.5 ml HCl, 1.5 ml HF) and followed by washed with running water and alcohol, and air dried for microstructural analysis. The hardness has been measured for the welds using Vickers's hardness tester. The vickers's hardness (HV) test was conducted across the cross section of the samples, at three different positions in welds.

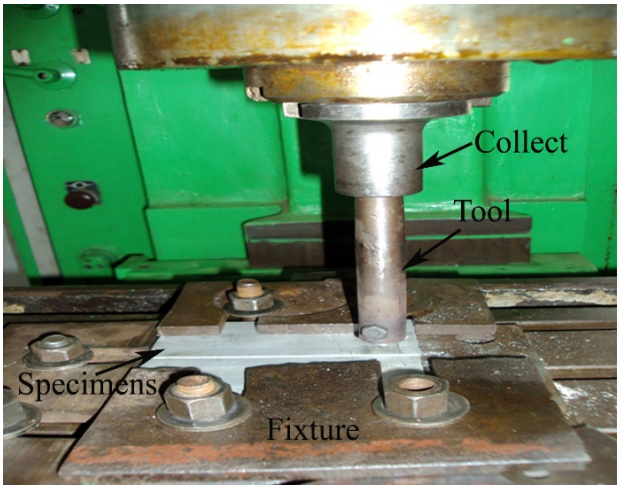

Fig. 1 A photograph of the clamping of the samples for friction stir welding.

Fig. 2 The image of the FSW tool used in the present study.

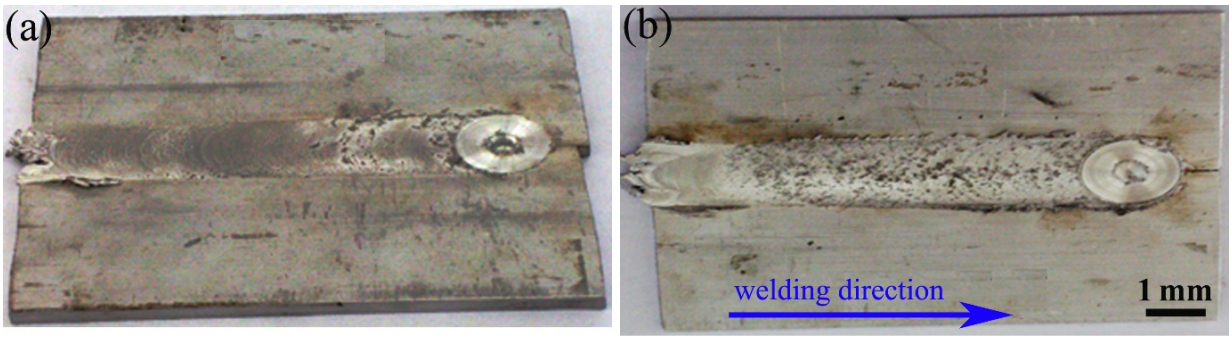

Fig. 3 The visual appearance of the friction stir welding joints with crown formation (a) water cooled (underwater welding) and (b) air cooled samples.

The mechanical properties of the joints were evaluated under universal testing machine UTE-40 with a capacity of 100 kN, India. The tensile samples were prepared as per the ASTM E8 standard. The tensile test was carried out at room temperature at a cross-head speed of 1.5 mm/min, and the tensile test results of each joint were evaluated using five tensile samples cut from the same joint. After completion of tensile tests the optical microscope and scanning electron microscope were used to analyze the microstructural features of the joints.

Results and Discussion

Microstructural Analysis. The friction stir welding of AA6061 aluminum alloys were welded under with water (WW) and without water (WOW) cooling using threaded pin. The pin geometry and diameter were found to be most significant effect on the tensile strength of the joints and cross sectional area owing to the stirring in the weld nugget is mainly caused by the action of the pin [12]. The visual inspection of the obtained welds with threaded pin characterized with the weld surface of roots and crowns. The weld quality information is always provided by the circle of material which is deformed by the friction stir welding tool shoulder. The appearance of the welds (see Fig. 3) exhibited a good weld with the circle around the exit hole is complete and the roots and crowns are formed appropriate. The friction stir welded joints performed under water and air can be seen that sound welds formation without obvious defects such as tunnel, cracks type defects was obtained for both the 1120 rpm and 1400 rpm rotational speeds with the tool pin moves along the center line of the butt weld. It is contrary to other researcher's reports that if tool rotating pin moves along the center line of the butt joint configuration cracks and other types of defects developed [38]. It is observed that water cooled friction stir welded joints produced a very little amount of flash than the air cooled joints with the formation of smooth crown and surfaces during process.

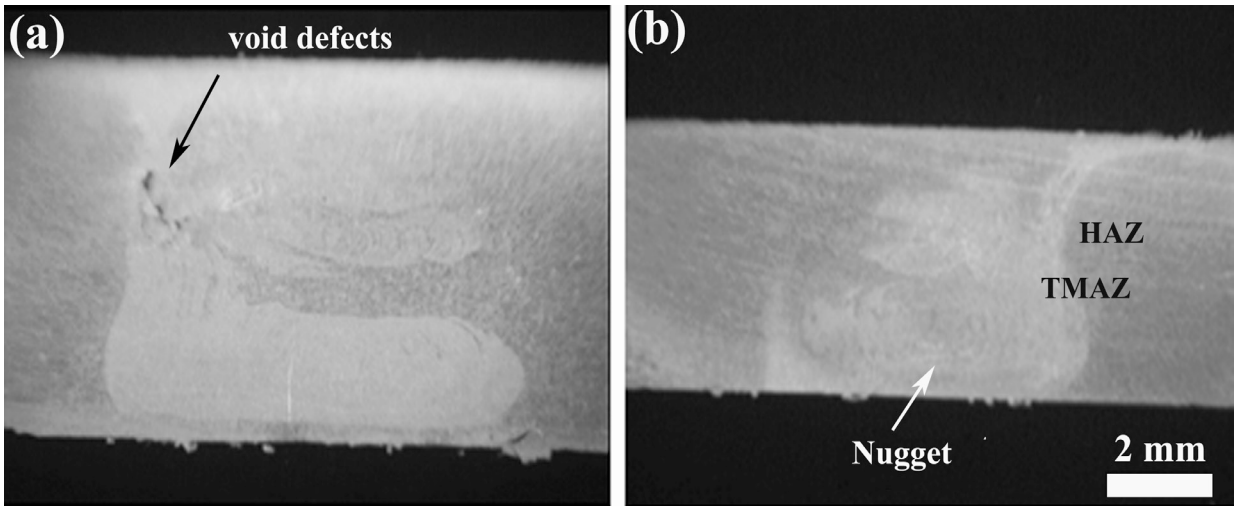

Fig. 4 Macrostructure showing the appearance of the friction-stir welded AA6061 joints at 1120 rpm (a) without water cooling, and (b) with water cooling.

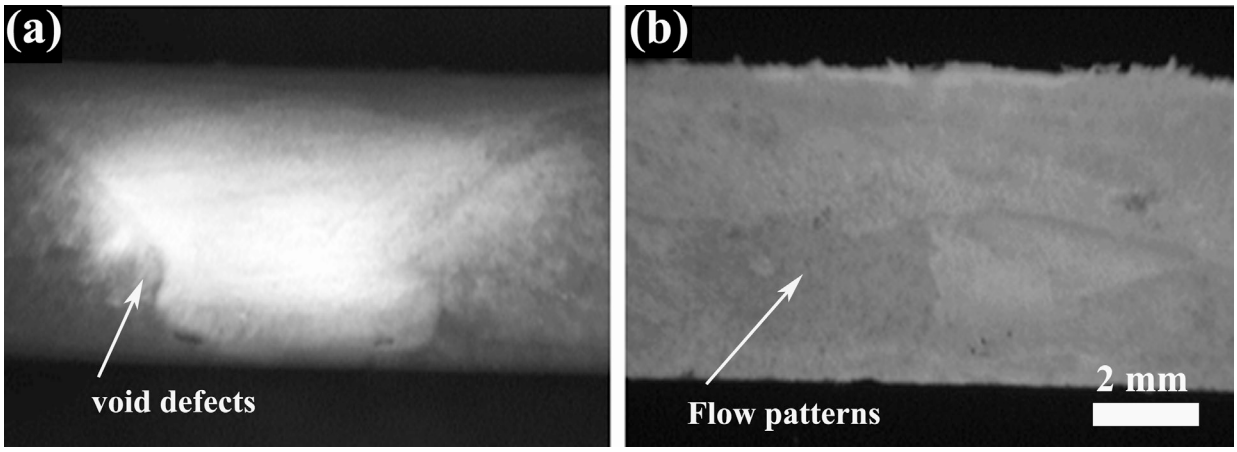

Fig. 5 Macrostructure showing the appearance of the friction-stir welded AA6061 joints at 1400 rpm (a) without water cooling, and (b) with water cooling.

The cross-sectional macrostructures of the joints of the FSWed joints produced at 1120 rpm are illustrated in Fig. 4. Under close observance of the microstructural analysis exhibits no welding defects for the underwater welding joints. Whereas, there are noticeable weld defects like voids and/or porous are formed in the air cooled joints (see Fig. 4a). It is also found that the nugget formation in the water cooled joints is evenly formed with the proper mixing in the stir zone. The ductilizing effect decreases with decreasing of temperature generation and a complex metal flow is not occurred in water cooled joints. Hence defect free macrostructure is formed for water cooling during welding. The upper part of the macrostructure of the air cooled joints characterized by severe plastic deformation of the aluminum alloys, but the lower part of the weld nugget shows a much smoother nugget formation and less intermixing. The previous research report showed the similar observations for the aluminum side in case of dissimilar joints between magnesium to aluminum [39]. The difference in microstructural formation between air cooled and water cooled joints mainly due to the changes in thermal history of the joints. In case of air cooled joints the variation for formation of lower part of the macrostructure owing to the flow field in friction stir welding which is most likely to form strong mixing on advancing side of the tool shoulder. The macrostructure of the FSWed joints with increased rotational speed from 1120 rpm to 1400 rpm are depicted in Fig. 5. The macrostructure of the 1400 rpm of air cooled joints exhibits better nugget formation than the joints at 1120 rpm. The nugget with small amount of defects and fully formed trapezoidal shape is formed. The defects formation in the stir zone with the cavity effect produced by the effect of rotational speed, the material flow on the advancing side was squeezed and brought to the back of the pin. Conversely, there is no two parts of the macrostructure formed and this is due to the pin and rotational speed influence on full nugget formation. While, the with water cooling joints at 1400 rpm rotational speed shows drastic change in their macrostructure formation. With increasing rotational speed from 1125 rpm to 1400 rpm, the nugget with onion rings shifted from the center of the stir zone to the upper part of the stir zone. Liu et al. [40], also observed the microstructural changes with the rotational speed and welding speed. In their study, it is found that the increase in welding speed from 400 to 600 mm/min results in shifting of onion rings from the middle of the stir zone to the top of the stir zone. It is also observed that, decreasing of tool rotation rate from 1400 rpm to 900 rpm resulted in dispersing of nugget boundary at the retreating side. The enlarged view of macrographs for the influence of rotation speed of 1120 rpm and 1400 rpm, are illustrated in Fig. 6. The macrostructure of the air cooled joints shows the improvement in nugget formation from 1120 rpm to 1400 rpm rotational speed. The increase in size of the stir zone with clear view of onion rings flow patterns formation can be seen for joints at 1400 rpm rotational speed (see Fig. 6b). The macrostructure formed under WOW cooled joints at 1400 rpm is represents a second mode of metal transfer. At low rotational speed a complex mode of metal flow can be occur due to the decrease in ductility of the stir zone. It is also found that WOW cooled joints reveals a wider thermo mechanical affected zone (TMAZ) in advancing side and retreating side which are higher than the WW cooled joints.

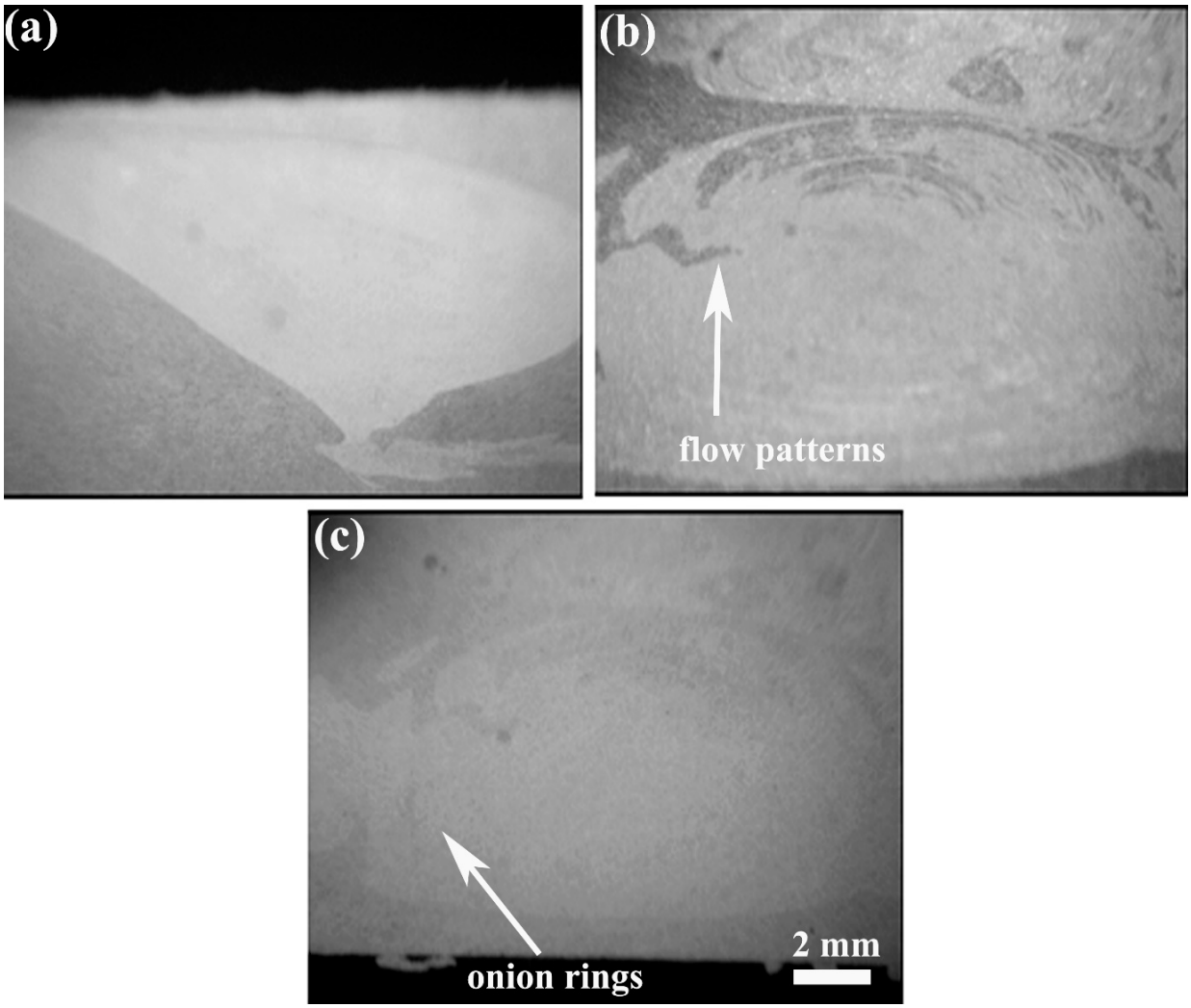

Fig. 6 The enlarged view of the macrostructures showing the effect of rotating speed on nugget shape formation WOW cooling (a) 1120 rpm (b) 1400 rpm and (c) 1400 rpm WW cooling.

However, the second mode and complex metal flows are diminished by applying critical cooling using under water welding with decreasing temperature, thus the joints produced without any defects in the weld zone. Figure 6(c) shows the macrostructure of the water cooled joints with defects formation and the material flow pattern of onion rings in the nugget. The tool shoulder moves a small quantity of metal as layer by layer from the high pressure side (advancing) to low pressure side (retreating). At the same time the remaining metal moves by the second mode of metal transfer. The mechanism of metal flow transfer in the first mode is compactness to the weld. As seen in Fig. 6(b), different macrostructure with metal flow patterns are due to different layers of metal moved by the first and second modes of metal transfer. The formation of onion rings in the nugget (see Fig. 6c) are based on two modes of metal transfer. In the first mode, pin stirs the metal as layer by layer parallel to the tool axis. In second mode, the shoulder brings the metal layer by layer perpendicular to the tool axis. Therefore, the onion rings pattern formation are owing to the collective effect of first and second modes of metal transfer [41].

The microstructural analysis of the joints FSWed at 1120 rpm without and with water cooled joints are presented in Fig. 7 and 8, respectively. It is characterized that three distinct microstructural zones, i.e., stir zone (SZ), thermo mechanically affected zone (TMAZ), and heat affected zone (HAZ) were discernible. Figure 7 shows the microstructures of base metal, TMAZ, HAZ and SZ of the samples of 1120 rpm rotational speed. Base metal microstructure has elongated grains coarser than the other zones. Whereas, the HAZ microstructure has grains less coarse than the base metal in the rolling direction and no distinct interface difference is observed between them.

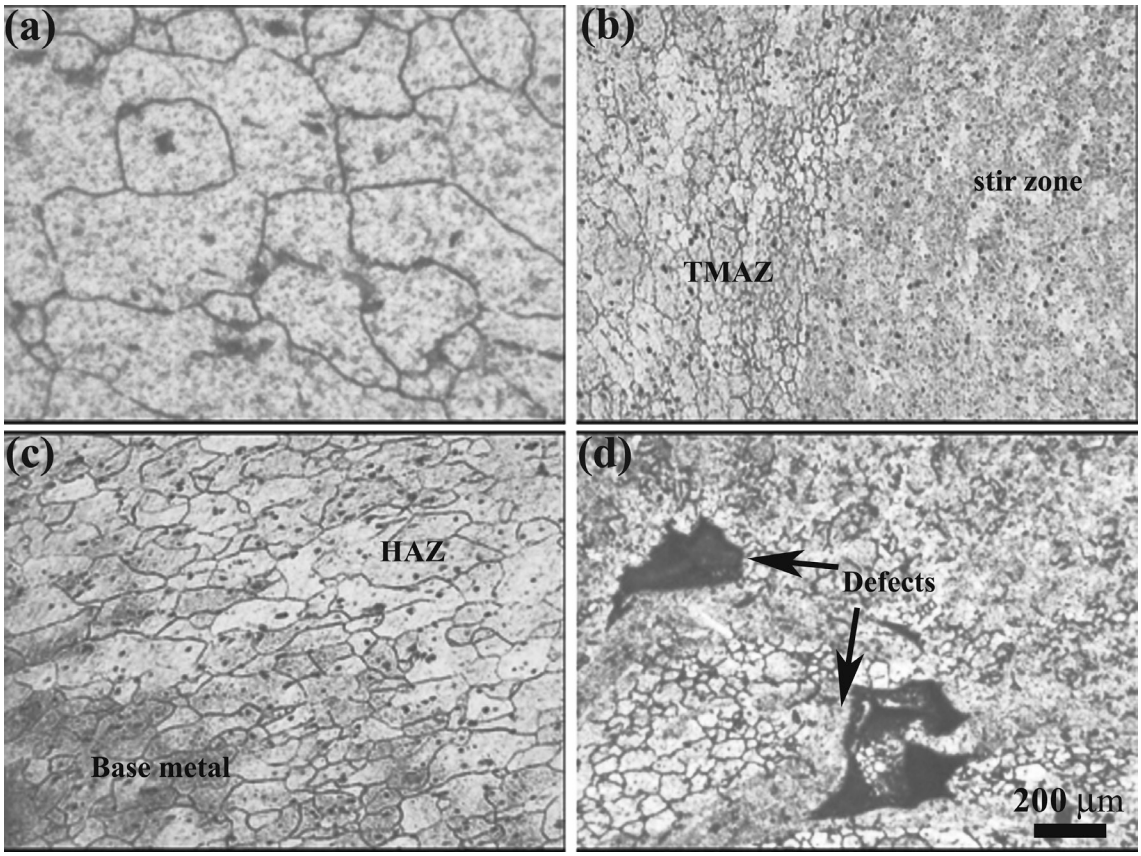

Fig. 7 Microstructures analysis of the joints at 1120 rpm without water cooling (a) base metal (b) weld interface between TAMZ and stir zone (c) weld interface between HAZ and base metal (d) defects formation at weld interface.

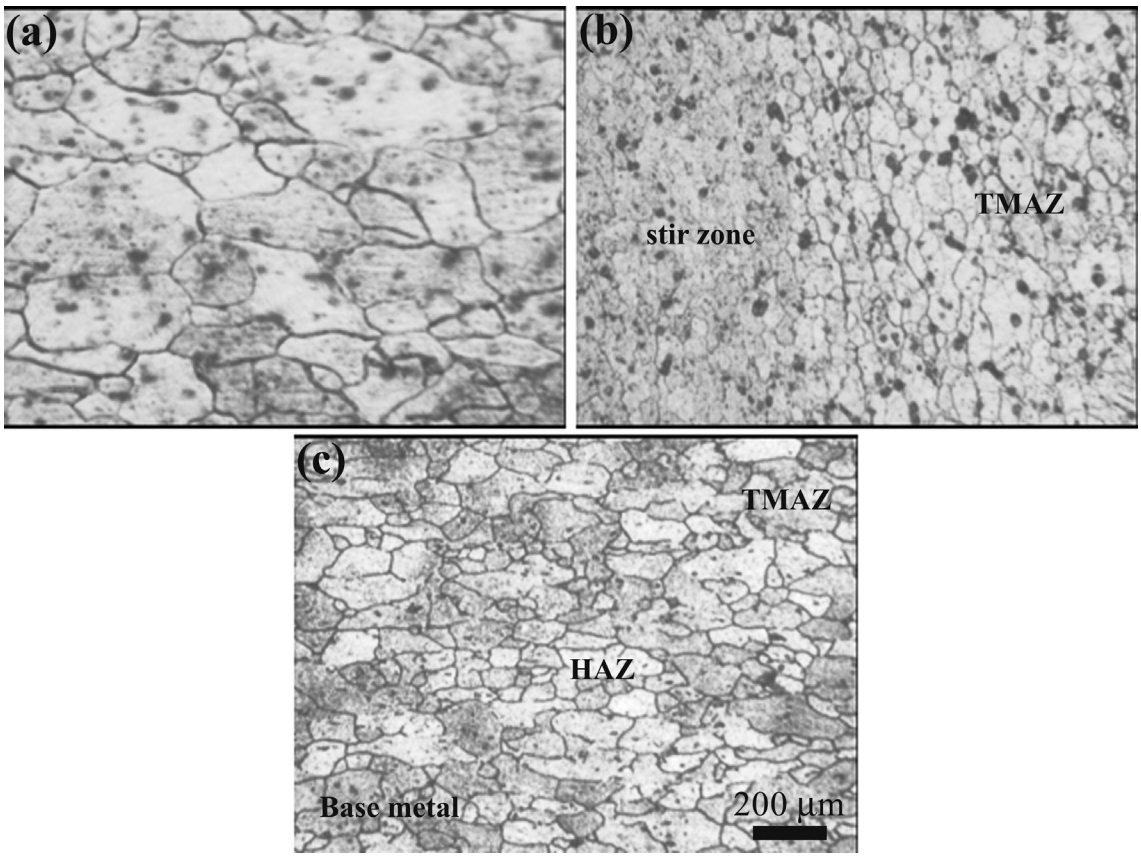

Fig. 8 Microstructure analysis of the joints at 1120 rpm with water cooling (a) base metal (b) weld interface between TAMZ and stir zone (c) weld interface between HAZ and base metal.

The grain size difference is in several hundred microns long and approximately HAZ grain size is half of the grain size of base metal. The deformed elongated grains are formed in an upward flowing perpendicular to HAZ and base metal microstructure pattern in the TMAZ, as shown in Fig. 7(b). However, the plastic deformation effect have little influence on the TMAZ, recrystallization did not occur in this zone because of insufficient rotational speed on deformation strain and thermal input for 1120 rpm joints. Whereas, the deformed grains are observed in TMAZ of 1400 rpm joints where the sufficient frictional deformation is occurred. In the same image it can be seen that the stir zone exhibited the fine and equiaxed grain structure, representing the formation of dynamic recrystallization due to the effect of pin rotation on severe plastic deformation and thermal input. The similar observations were characterized and found that the average grain size of the stir zone was 12 µm formed due to dynamic recrystallization effect [40]. The base metal plastic deformation direction is showing consistent with the welding direction and comparatively a relative deformation difference formed between base metal and the plastic deformed metal. So the weld interface between the nugget zone and TMAZ is obvious. The flow patterns of the plasticity deformed metal on the retreating side flow to the back side of the pin and the deformation grains/material direction of base metal is conflicting to the welding direction. There is no obvious interface formation between the nugget zone and the TMAZ from the retreating side other than the base metal plasticity deformed metal on retreating side [42]. Figure 7 (d) illustrates the defects formation in the weld nugget with the size of approximately 500 µm width. As explained in earlier, defects formation due to the insufficient rotation speed hence the low heat input formed in the weld. The microstructures of the joints with different zones HAZ, TMAZ, SZ and base metal of the welds with water cooling are shown in Fig. 8. The characterization of the under welded microstructural observations revealed that the features are almost similar to without water cooled welds expect the grain size difference and defects formation. The microstructures are very fine and equiaxed grains in both the welding conditions of stir zone. A large variation in grain size and its distribution is observed for different travel speeds and the microstructures of the welds appears to be recrystallized up to 32 mm/min. It is worth to mention that the nugget microstructure appears more fine and uniform with the increasing of the rotational speed and travel speed. It seems to be that increasing of speed results in the combination of hot working and dynamic recovery and recrystallization is optimal for the desired conditions. It is observed that there is an increase in the peak temperature with increasing the revolutionary pitch and the influence of travel speed (at the same tool rotation speed) on the material mixing. To see the effect of speed, it is related to the welding conditions of such parameters to the resultant mean grain size. The decrease in temperature of the nugget zone denotes the axial force acting on the weld line is not sufficient to form a plastic flow to achieve the dynamic recrystallization process. While, increase in temperature of the material for the low travel speed at the same rotational speed, material is extremely softened and can be grain growth after deformation.

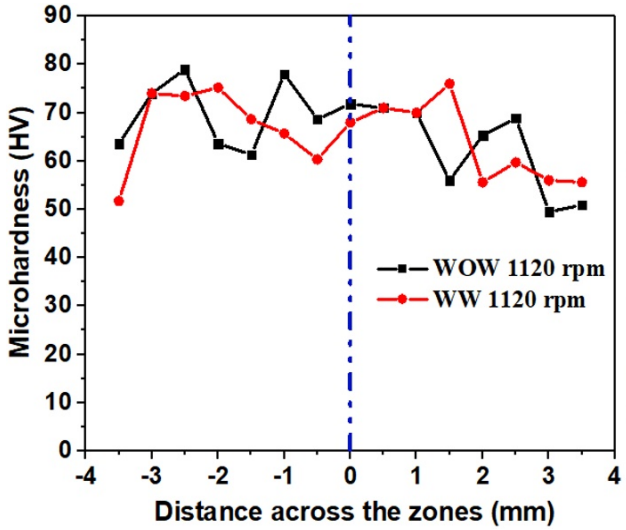

Fig. 9 Microhardness of the welds at different welding conditions.

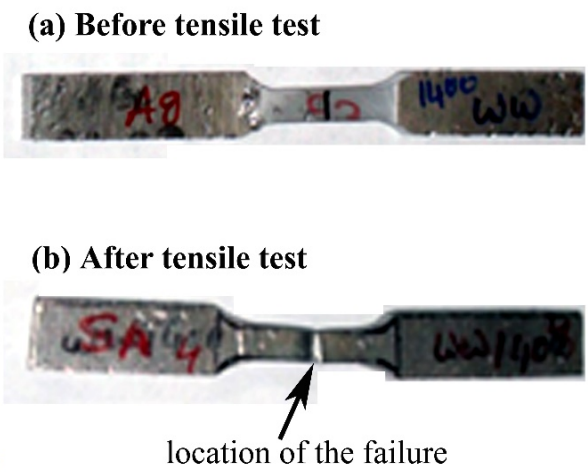

Fig. 10 Visual appearance of the tensile samples (a) before testing (b) after testing.

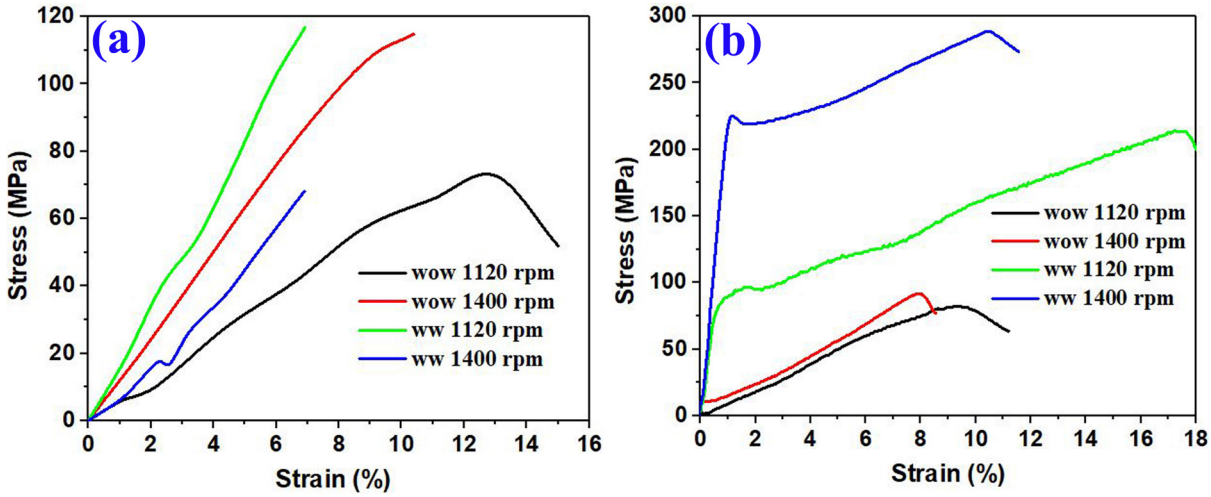

Fig. 11 Tensile strength of the joints at different welding conditions (a) solutionized at 540 ˚C for 1 hour (b) ageing at 160 ˚C for 8 hours.

Mechanical Properties. Vickers micro hardness values are measured along the weld cross section of the joints at 1120 rpm with and without water cooling, are plotted in Fig. 9. The micro hardness distributions in the three zones such as FSW of HAZ, TMAZ, stir zone and base metal are taken to identify the weakest region of the weld metal. It is observed that the variation in overall values of the hardness across the three zones is not so high, but significantly has variation to discuss. The weld nugget has a very fine recrystallized grain structure, with hardness values between 60 and 68 HV. Whereas, outside of the nugget adjacent to stir zone, the thermo-mechanically affected zone consists of highly elongated and deformed grains, which comprise the hardness values of 70-75 HV. In overall, the hardness of the water cooled joints higher than the air cooled joints. This is due to the refined grain structure formation in the underwater welds than the air cooled and base metal grain structure. From the microstructural analysis it is correlated that, the precipitates in the low hardness region of air cooled joints are significantly coarsened during friction stir welding, which has more influence on the decreasing of hardness. Whereas, in case of underwater FSWed joints, although the precipitates are diffused into the metal, the welding thermal cycles can produce the high density dislocations which are formed as seen in previous studies [43]. However, the dissolution of precipitates in the matrix is more beneficial to the solid solution strengthening. Hence, the more refined fine grain structures, solid solution strengthening effect and dislocation density are greatly contributes the increase of micro hardness and therefore enhance the tensile strength of the underwater FSWed joints [44].

The tensile strength of FSWed air cooled and water cooled joints are evaluated to observe the efficiency of the joints. It is found that the tensile samples failed in weld center where the hardness gradient becomes varied (as seen in Fig. 9.) and tensile samples before and after tensile testing are shown in Fig. 10. The welds obtained with water cooling shows better tensile properties when compared to the welds obtained without water cooling. The FSWed joints of the precipitation-strengthened Al alloys, the fracture of the tensile specimens occurred at the center of the welds adjacent to the HAZ (partly in TMAZ), which is weakest zone of the welds [45]. The similar studies have been indicated that the fracture path of the FSWed AA6061 joints was consistent with the formation of lowest hardness [46]. It demonstrates that while the joint failure zone consistent to the tensile axis of the FSWed AA6061 joints were controlled by the low hardness zone formation, and the tensile strength can be directly determined by the hardness values of the low hardness zone of the joints. The joints are heat treated at different conditions to enhance the mechanical properties of the joints. The super imposed stress-strain curves of the tensile tests conducted at different rotational speed of with and without water cooled joints, are illustrated in Fig. 11. The tensile strength, percentage of elongation, yield strength and joint efficiency of the welds varying with the different heat treatment conditions i.e, solutionized at 540 ˚C for 1 hour (see Fig. 11a) and ageing at 160 ˚C for 8 hours (see Fig. 11b). The maximum tensile strength measured as 288 MPa for under water joints at ageing conditions, the yield strength of 111 MPa and joint efficiency of 89.87%. The

joint efficiency was measured for each sample to evaluate the strength recovery in each sample by calculating the ratio of tensile strength of joints to the tensile strength of the parent metal. The joints yield strength after PWHT showed a dropping level along the depth of the joint. In case of joints under PWHT of solutionized at 540 ˚C for 1 hour showed similar trend for ultimate tensile strength and maximum strength obtained for 120 MPa. It is also observed that, increasing in welding speed resulted in both ultimate tensile strength and joint efficiency increases. Cavaliere et al. [47] also found the similar observations for the increase in tensile strength with the increasing of welding speed of the tool for dissimilar combinations. It has been reported that heat input generation in the welds by the tool shoulder is an important factor in FSW process, and also, the properties of the joints are strongly influenced by this factor. In addition, the heat input generation is directly dependent on the tool rotational speed. It is observed that the yield stress of the joints is less than that of the base metal, while the weld metal yield stress slightly decreases as the enforced heat input increases. As per the aforementioned results of microstructures and hardness values, the improved tensile strength of the friction stir welded joints produced at higher welding speed is mainly due to the condensed dissolution of precipitates due to the low heat generation in the weld length during friction stir welding. Whereas, the PWHT welds results in the formation of precipitate particles during aging process. A large increase in strain was observed for the heat treated joints produced at low welding speed (see Fig. 11a&b). In case of the joints produced at low speed 1120 rpm of without water cooling joints solutionized at 540 ˚C for 1 hour and with water cooling joints ageing at 160 ˚C for 8 hours, are observed to be have higher ductility than the as welded and other heat treated joints. The increase in ductility of the joints owing to the FSW process softens the welds significantly which in turn lowers the tensile strength and increases the ductility of the welded joints. The occurrence of this phenomena may be attributed to the decreasing of preexisting dislocations and elimination of strengthening precipitates [47, 48]. It is also found that the initial strength of the substrates is never reached during subsequent natural ageing, however, the strength of the artificially aged welds is higher than that of the base metal. It may be owing to the effect of grain refinement in the weld nugget that enhances the nucleation rate, therefore, it produces a very fine and equiaxed distribution of strengthening precipitates. It is worth to note that the as welded and partially the samples produced with ageing at 160 ˚C for 8 hours have an serrated flow, while this effect is not appeared for samples produced with solutionized at 540 ˚C for 1 hour (see Fig. 11a&b). It is expecting that the possible reason for formation of this flow because of the reducing of dislocations by in-solution substantial atoms during tensile test [27, 49]. As explained earlier that, during the FSW process partial solution treatment takes place thus resulted in formation of supersaturated substantial solid solution. From the above observations it is expecting the effect of Portevin-Le Chatelier to be operative for as welded and ageing at 160 ˚C for 8 hours welds, whereas at higher temperature heat treatment conditions of solutionized at 540 ˚C for 1 hour which is employed in this work, shows the substantial atoms of Mg have participation in precipitated process. Therefore, the Portevin-Le Chatelier serrations effect disappeared owing to the formation of new strengthening precipitates. As shown in Fig. 10, tensile failure in the sample occurs in advancing side of the HAZ and TAMZ regions, where a sudden change in hardness distribution values is observed agreeing to Fig. 9. It is also agreed with the Figures 7 and 8, which shows the changes in microstructural formations with the grain size variations of various zones of the weld nugget. However, the fracture in the tensile samples for various conditions took place almost in the same regions even though the underwater welded joints after ageing achieved the highest strength than the without water cooled FSWed joints.

Conclusions

Friction stir welds of AA6061 were produced in with (underwater) and without (air) water cooling using various rotational speeds. The stir zone of without water cooled joints displayed complex material flow patterns with the presence of defects. Whereas, there is no defects are identified for the joints underwater welds. The coarsening grain structure and dissolution of precipitates formation in TMAZ as represents weakest zone. The thermal gradient in the joint can

be controlled by the underwater cooling thus strengthen of weaker zones such as HAZ and TMAZ. Therefore the reduction of HAZ width and over aging conditions are improves the tensile properties. The hardness distribution in TMAZ and HAZ is around from 70 HV to 76 HV for both underwater and air cooled joints. The joints of underwater welded samples with the PWHT ageing conditions are exhibited higher tensile strengths of 288 MPa and higher joint efficiency of 89.87% in contrast to air cooled joints. It is understood that, thermal histories of the welds and its subsequent PWHT effect on precipitation behavior are contributes greatest influence on the enhancement in the mechanical properties of underwater friction stir welded joints.

References

[1] R.A. Sielski, Research needs in aluminum structure, Ships. Offshore. Struc. 3(1) (2008), 57-65.

[2] H. Aydın, A. Bayram, A. Ugˇuz, K.S. Akay, Tensile properties of friction stir welded joints of 2024 aluminum alloys in different heat-treated-state, Mater. Des. 30 (2009) 2211-2221.

[3] A. Ambroziak, M. Korzeniowski, P. Kustroń, M. Winnicki, P. Sokołowski, E. Harapińska, Friction welding of aluminium and aluminium alloys with steel, Adv. Mater. Sci. Eng. 2014 (2014) 1-15.

[4] C.H. Muralimohan, V. Muthupandi, K. Sivaprasad, The influence of aluminium intermediate layer in dissimilar friction welds, Inter. J. Mater. Res. 105 (2014) 350-357.

[5] S.S. Kumaran, S. Muthukumaran, D. Venkateswarlu, G.K. Balaji, S. Vinodh, Eco-friendly aspects associated with friction welding of tube-to-tube plate using an external tool process, Int. J. Sustainable. Eng. 5 (2012) 120-127.

[6] C.H. Muralimohan, S. Haribabu, Y.H. Reddy, V. Muthupandi, K. Sivaprasad, Joining of AISI 1040 steel to 6082-T6 aluminium alloy by friction welding, J. Adv. Mech. Eng. Sci. 1(1) (2015) 57-64.

[7] M. Cheepu, V. Muthupandi, B. Srinivas, K. Sivaprasad, Development of a friction welded bimetallic joints between titanium and 304 austenitic stainless steel, in: P.M. Pawar, B.P. Ronge, R. Balasubramaniam, S. Seshabhattar (Eds.), Techno-Societal 2016, International Conference on Advanced Technologies for Societal Applications, ICATSA 2016, Springer, Cham, 2018, pp 709-717. https://doi.org/10.1007/978-3-319-53556-2_73

[8] C.H. Muralimohan, S. Haribabu, Y.H. Reddy, V. Muthupandi, K. Sivaprasad, Evaluation of microstructures and mechanical properties of dissimilar materials by friction welding, Procedia. Mater. Sci. 5 (2014) 1107-1113.

[9] T. Osada, K. Sonoya, T. Abe, M. Nakamura, Developing of the aluminum alloy solid state bonding method in atmosphere using high frequency induction heating and ultrasonic vibration Uni. J. Mech. Eng. 4 (2016) 1-7.

[10] A.A. Shirzadi, E.R. Wallach, New approaches for transient liquid phase diffusion bonding of aluminium based metal matrix composites, Mater. Sci. Technol. 13 (1997) 135-142.

[11] P.L. Threadgill, A.J. Leonard, H.R. Shercliff, P.J. Withers, Friction stir welding of aluminium alloys, Int. Mater. Rev. 54 (2009) 49-93.

[12] D. Venkateswarlu, N.R. Mandal, M.M. Mahapatra, S.P. Harsh, Tool design effects for FSW of AA7039, Weld. J. 92 (2013) 41-47.

[13] A. Kumar, M.M. Mahapatra, P.K. Jha, N.R. Mandal, V. Devuri, Influence of tool geometries and process variables on friction stir butt welding of Al-4.5%Cu/TiC in situ metal matrix composites Mater. Des. 59 (2014) 406-414.

[14] B.S. Yigezu, D. Venkateswarlu, M.M. Mahapatra, P.K. Jha, N.R. Mandal, On friction stir butt welding of Al + 12Si/10 wt% TiC in situ composite, Mater. Des. 54 (2014) 1019-1027.

[15] H.K. Mohanty, D. Venkateswarlu, M.M. Mahapatra, P. Kumar, N.R. Mandal, Modeling the effects of tool probe geometries and process parameters on friction stirred aluminium welds, J. Mech. Eng. Autom. 2(4) (2012) 74-79.

[16] D. Venkateswarlu, P.N. Rao, M.M. Mahapatra, S.P. Harsha, N.R. Mandal, Processing and optimization of dissimilar friction stir welding of AA 2219 and AA 7039 alloys, J. Mater. Eng. Perform. 24(12) (2015) 4809-4824.

[17] V. Devuri, M.M. Mahapatra, S.P. Harsha, N.R. Mandal, Effect of shoulder surface dimension and geometries on FSW of AA7039, J. Manuf. Sci. Prod. 14 (2014) 183-194.

[18] F. Grignon, D. Benson, K.S. Vecchio, M.A. Meyers, Explosive welding of aluminum to aluminum: analysis, computations and experiments, Int. J. Impact. Eng. 30 (2004) 1333-1351.

[19] A.H.M.E. Rahman, M.N. Cavalli, Strength and microstructure of diffusion bonded titanium using silver and copper interlayers, Mat. Sci. Eng. A. Struct. **527**5 (2010) 189-193.

[20] M.M. Cheepu, V. Muthupandi, S. Loganathan, Friction welding of titanium to 304 stainless steel with electroplated nickel interlayer, Mater. Sci. Forum. 710 (2012) 620-625.

[21] C.H. Muralimohan, M. Ashfaq, R. Ashiri, V. Muthupandi, K. Sivaprasad, Analysis and characterization of the role of Ni interlayer in the friction welding of titanium and 304 austenitic stainless steel, Metall. Mater. Trans. A. 47 (2016) 347-359.

[22] C.H. Muralimohan, V. Muthupandi, Friction welding of type 304 stainless steel to CP titanium using nickel interlayer, Adv. Mater. Res. 794 (2013) 351-357.

[23] C.H. Muralimohan, V. Muthupandi, K. Sivaprasad, Properties of friction welding titanium-stainless steel joints with a nickel interlayer, Procedia. Mater. Sci. 5 (2014) 1120-1129.

[24] M. Cheepu, M. Ashfaq, V. Muthupandi, A new approach for using interlayer and analysis of the friction welding of titanium to stainless steel, Trans. Indian. Inst. Met. (2017). https://doi.org/10.1007/s12666-017-1114-x

[25] W.M. Thomas, E.D. Nicholas, J.C. Needham, M.G. Murch, P. Temple-Smith and C.J. Dawes, Friction stir butt welding, GB patent 9125978.8. (1991).

[26] P.M.G.P. Moreira, T. Santos, S.M.O. Tavares, V. Richter-Trummer, P. Vilaça, P.M.S.T. de Castro, Mechanical and metallurgical characterization of friction stir welding joints of AA6061-T6 with AA6082-T6, Mater. Des. 30 (2009) 180-187.

[27] H. Jamshidi Aval, S. Serajzadeh, A study on natural aging behavior and mechanical properties of friction stir-welded AA6061-T6 plates, Int. J. Adv. Manuf. Technol. 71 (2014) 933-941.

[28] G. Çam, Friction stir welded structural materials: beyond Al alloys, Int. Mater. Rev. 56 (2011) 1-48.

[29] S. Malarvizhi, V. Balasubramanian, Influences of welding processes and post-weld ageing treatment on mechanical and metallurgical properties of AA2219 aluminium alloy joints, Weld. World. 56 (2012) 105-119.

[30] L.E. Murr, G. Liu, J.C. Mcclure, A TEM study of precipitation and related microstructures in friction-stir-welded 6061 aluminium, J. Mater. Sci. 33 (1998) 1243-1251.

[31] A.K. Lakshminarayanan, V. Balasubramanian, K. Elangovan, Effect of welding processes on tensile properties of AA6061 aluminium alloy joints, Int. J. Adv. Manuf. Technol. 40 (2009) 286-296.

[32] S. Lim, S. Kim, C.G. Lee, S. Kim, Tensile behavior of friction stir-welded Al 6061-T651, Metall. Mater. Trans. A. 35 (2004) 2829-2835.

[33] K.N. Krishnan, The effect of post weld heat treatment on the properties of 6061 friction stir welded joints, J. Mater. Sci. 37 (2002) 473-480.

[34] S. Malarvizhi, V. Balasubramanian, Effects of welding processes and post-weld aging treatment on fatigue behavior of AA2219 aluminium alloy joints, J. Mater. Eng. Perform. 20 (2011) 359-367.

[35] G. İpekoğlu, S. Erim, B. Gören Kıral, G. Çam, Investigation into the effect of temper condition on friction stir weldability of AA6061 Al-alloy plates, Kovove. Mater. 51 (2013) 155-163.

[36] G. İpekoğlu, S. Erim, G. Çam, Investigation into the influence of post-weld heat treatment on the friction stir welded AA6061 Al-alloy plates with different temper conditions, Metall. Mater. Trans. A. 45 (2014) 864-877.

[37] H.J. Zhang, H.J. Liu, L. Yu, Effect of water cooling on the performances of friction stir welding heat-affected zone, J. Mater. Eng. Perform. 21 (2012) 1182-1187.

[38] J. Yan, Z. Xu, Z. Li, L. Li, S. Yang, Microstructure characteristics and performance of dissimilar welds between magnesium alloy and aluminum formed by friction stirring, Scripta. Mater. 53 (2005) 585-589.

[39] M.A. Mofid, A. Abdollah-zadeh, F.M. Ghaini, The effect of water cooling during dissimilar friction stir welding of Al alloy to Mg alloy, Mater. Des. 36 (2012) 161-167.

[40] F.C. Liu, Z.Y. Ma, Influence of tool dimension and welding parameters on microstructure and mechanical properties of friction-stir-welded 6061-t651 aluminum alloy, Metall. Mater. Trans. A. 39A (2008) 2378-2388.

[41] S. Muthukumaran, S.K. Mukherjee, Two modes of metal flow phenomenon in friction stir welding process, Sci. Technol. Weld. Join. 11 (2006) 337-340.

[42] Y. Zhao, Z. Lu, K. Yan, L. Huang, Microstructural characterizations and mechanical properties in underwater friction stir welding of aluminum and magnesium dissimilar alloys, Mater. Des. 65 (2015) 675-681.

[43] J.Q. Su, T.W. Nelson, R. Mishra, M. Mahoney, Microstructural investigation of friction stir welded 7050-T651 aluminium, Acta. Mater. 51 (2003) 713-729.

[44] L. Hui-jie, Z. Hui-jie, H. Yong-xian, Y. Lei, Mechanical properties of underwater friction stir welded 2219 aluminum alloy, Trans. Nonferrous Met. Soc. China. 20 (2010) 1387-1391.

[45] A. Scialpi, L.A.C. De Filippis, P. Cavaliere, Influence of shoulder geometry on microstructure and mechanical properties of friction stir welded 6082 aluminium alloy Mater. Des. 28 (2007) 1124-1129.

[46] S.R. Ren, Z.Y. Ma, L.Q. Chen, Effect of welding parameters on tensile properties and fracture behavior of friction stir welded Al– Mg–Si alloy, Scripta. Mater. 56 (2007) 69-72.

[47] P. Cavaliere, A.D. Santis, F. Panella, A. Squillace, Effect of welding parameters on mechanical and microstructural properties of dissimilar AA6082-AA2024 joints produced by friction stir welding, Mater. Des. 30 (2009) 609-616.

[48] S. Kou, Y. Le, Nucleation mechanism and grain refining of weld metal, Weld. J. 65(4) (1986) 65-70.

[49] E.O. Hall, Yield point phenomena in metals and alloys, Plenum Press, New York, 1970.